Comparison of the Melting Behavior of HDPE and PP in Single Screw Extruders

Modified on Friday, 01 May 2015 04:05 PM by mpieler — Categorized as: Paper of the Month

Comparison of the Melting Behavior of HDPE and PP in Single Screw Extruders

María del Pilar Noriega, Tim A. Osswald and Alberto Naranjo*
ICIPC – Plastics and Rubber Institute
Carrera 49 No. 5 Sur-190, Medellin, Colombia, South America

**Polymer Engineering Center (PEC), Department of Mechanical Engineering*
University of Wisconsin-Madison, Madison, Wisconsin 53706

Abstract

Actual experimental techniques designed to study melting behavior of polymers inside the screw extruder suffer from lack of functionality and high time consuming procedures. Their invasive nature affect friction characteristics and heat transfer, influencing the outcome of measured parameters. This paper presents a patented technique (U.S Patent No. 7314363) that can capture experimental data and images from inside the extruder at short response times using a highly instrumented 45 mm extruder with built-in sensors and small quartz windows. The melting behavior of polyethylene and polypropylene were visualized and measured with this non-invasive technique. A comparison of the melting behavior of both polymers was obtained.

Background

Maddock and Street carried out their experiments using a polymer with a high degree of crystallinity (polyethylene). From observation of the solidified content of the screw channel a qualitative description of the melting mechanism could be given. The experimental technique consisted of abruptly stopping an extruder operating at steady state, chilling both barrel and screw, pushing out the screw from the barrel, unwinding the polymer from the screw and slicing thin representative sections perpendicular to the flights. To better visualize the process, a small amount (3 – 5 %) of colored polymer was added as a tracer to distinguish between the solid and the molten regions. The experiments also provided some information on flow patterns, [1, 2]. The model, which they proposed, describes the melting as a process of which the major part of the heat transfer takes place through a thin molten layer, which is formed, at the hot extruder barrel. Under the condition that the thickness of the film exceeds the width of the clearance between the flight and the barrel surface, the melt film will be removed by the advancing screw flight. A pool of molten polymer is formed at the pushing side of the flight. The scraped-off melt is mixed with previously molten material due to the circulatory flow in this pool, caused by the component of the barrel velocity perpendicular to the flight.

Tadmor developed a quantitative model based on the experimental results of Maddock. As previously mentioned, the solid bed is pushed against the trailing flight flank. Between the solid bed and the barrel is a relatively thin melt film. Material melting at the solid/melt interface enters into this melt film and is dragged toward the leading flight flank where the majority of the melt collects in the melt pool, [3, 4]. Most melting occurs at the interface between the solid bed and the melt film between the solid bed and the barrel. Melting occurs as a result of the heat conducted from the barrel and viscous heat generation in the melt film. The latter is high because of the high shear rate in the melt film. The high shear rate is due to the high relative velocity between the barrel surface and the solid bed, [5]. This model was evaluated by conducting a series of experiments. Tadmor and coworkers were able to visualize, flow pattern or circulation in the melt pool and melt film by cooling down the extruder barrel, followed by removal of the barrel from the screw. The model was used to predict the solids bed profile (SBP) in screw channels of typical extruders.

Pearson and coworkers presented a complete analytical melting model assuming that the solid bed was not able to stand large differences of principal stresses and so account has to be taken explicitly of the downstream force balance on the solid bed and in the melt pool. He was the first one to divide the material in the screw channel into five zones. The zones were marked A, B, C, D and E. Zone A is the bed of solid polymer granules surrounded on all four sides by molten polymer. The solid material constitutes a freely flowing bed of granules. The existence of zones D and E depends on the temperature of the screw. Zone C is the thin melt layer zone, or melt film, and B is the melt pool as used in the previously described models. Melting takes place at all four interfaces, AB, AC, AD and AE. The viscous heat dissipation in the film was not considered in this model, [6, 7, 8, 9].

Wong, Zhu and coworkers studied the dynamic characteristics of the breakup of the solid bed during the melting process in a single screw extruder. Their observations confirmed that as a result of the increasing pressure gradient in the screw channel, the stresses exerted on the solid bed exceed the mechanical strength of the bed itself. In their research they found the solid bed strength as a function of bed temperatures, [10, 11]. They carried out their experiments in an extruder with its barrel equipped with glass windows or ‘glass extruder’. Derezinski developed a melting rate function based on the performance data of operating extruders to establish average general terms of the energy equation /12/.

Other Authors have investigated extensions of the above mentioned melting mechanisms or studied new melting mechanisms like dispersed solids melting, dissipative melting and mix-melting, [13, 14, 15]. These mechanisms have been found more suitable for twin screw extruders rather than single screw extruders. Dispersed solids melting (DSM) is considerably more efficient and the melting time is significantly shorter than contiguous solids melting [16].

Experimental

Optical Technique for In-Line-Measurement of Polymer Melting:

The main focus of the present research is the process visualization based on remote viewing into small diameter inside the extruder barrel. The first step in designing the process was to select and characterize a suitable optical setup, which could detect the phase change based on the differences in the density and optical properties of the polymer. This selection was a major step in the success of the visualization.

Three remote viewing possibilities were investigated including some of the following components like lenses, rod optics, fiber optics, illumination and color video systems:
- A micro-camera or lipstick camera of ⌀ 7 mm with flexible fiber optic light guide and illuminator,
- A flexible fiberscope of ⌀ 8 mm with a videolight source combination unit, and

A rigid boroscope of ⌀ 8 mm with fiber optic light guide and cold light source.

All the three possibilities required a special holder to locate the instrument in the extruder barrel. The function of the holder is to preserve the instrument at high processing temperatures and high extruder pressures. It is also clear that the holder is a mini-heat exchanger because it should keep the instrument at its operating temperature. The holder tip is a circular quartz window in contact with the polymer inside the extruder barrel for allowing visualization. Its geometry is ⌀ 10 mm ± 0.05 mm and thickness of 6 mm ± 0.05 mm. Fig. 1 shows the final holder concept and design after several heat transfer calculations and trials. The main holder components are: the shell, the core and the circular quartz window. The shell was manufactured in stainless steel of 300 series and has welded inlet and outlet for air cooling. For viewing into very small, straight and restricted areas, rigid boroscopes with rod lenses produce exceptionally clear images and they are less expensive than fiberscopes. A rigid boroscope of ⌀ 8 mm was selected considering optical coverage, holder geometry and holder locations every 2D along the extruder barrel. The operating temperature of a micro-camera system is in the range between – 10 °C and 40 °C due to the camera plastic sheathing. This low temperature resistance discarded this possibility. Fig. 2 shows a photograph of the new extruder setup showing the boroscope, illuminator, holders at different L/D positions along the barrel and the air cooling system.

Calibration:
The calibration of the whole optical setup was also a very important topic to be addressed in the present research. The purpose of calibration is to determine the relationship between image quantities (pixels) and the scene that is being imaged. Calibration ensures that measurements obtained from images can be used to accurately infer measurements of observed processes. In our application, the scene to be imaged is at a fixed distance from the camera (or rather, from the objective lens) and is roughly parallel to the image plane. These constraints make the calibration process simpler than "generic" camera calibration, [17]. The involved optics in the present In-Line technique requires a circular quartz window, several rod lenses inside the boroscope and the video camera lens. The distance object-lens was kept constant for all the experiments as needed. The only quantity of interest here involves the measurement of length; hence, the determination of the relationship between pixels and units of length (mm) at the several extruder barrel positions to be imaged is required. A simplified calibration procedure was developed. The accuracy of the results was verified by comparing the measured screw flight width with a caliper vs. the length of the screw flight measured with the optical setup. The obtained relationship between pixels and units of length was 1 mm = 129.884 pixels. Finally the conversion factor k is equal to 0.031 mm/pixel. This value is in the range of other similar optical systems between 0.01 and 0.035 mm/pixel, [17]. The accuracy of the obtained results was verified by comparing the screw flight width, e = 4.5 mm, vs. the length of the screw flight measured from the image. The obtained length was 610.23 pixels equivalent to 4.69 mm. There is an acceptable error of 4 %.

Fig. 3 shows the type of images to be analyzed and measured in this polymer melting research in single screw extruders. From left to right, the solid bed, melt pool, screw flight, narrow melt layer and solid bed can be clearly observed in the obtained image.

Results

Some images were captured from videos for illustration of the present research. For example, at 10 rpm four videos were recorded at barrel positions, 6D, 8D, 10D and 12D. Further videos were not recorded because the HDPE and PP materials were completely molten at 12 D. Two videos per barrel position (L/D) were recorded checking for reproducibility. Observations from both videos were the same.

Two images for HDPE at 6D were captured from the video on both sides of the screw flight and they are shown in Fig. 4.

The material flow direction was from the right to the left. As expected the HDPE and PP materials were completely solid and the polymer granules and screw flight were noticeable. Considering the solids bed profile, this measurement is equivalent to X/W = 1 after Tadmor nomenclature. Fig. 8 shows two images for PP at 6D.

Two images for HDPE at 8D were extracted from the video on both sides of the screw flight and they are presented in Fig. 5. As expected the HDPE material was partially molten and the polymer granules were compacted to a solid bed. The left picture showed the melt pool and the screw flight and the right picture showed the screw flight, narrow gap of molten polymer and the compacted solid bed. The solid bed appeared white and opaque, while the molten material appeared transparent; therefore the screw root was observable. The narrow gap of molten polymer on the right picture of Fig. 5 was not clear and reproducible observed in Tadmor 'pushout' or cooling experiments, [18]. Pearson and coworkers described this situation in their model. The screw flight was always clear in all the images. Considering the SBP, this measurement is equivalent to X/W < 1. On the contrary, the PP material at 8D was still solid with rubbery appearance and the polymer granules and screw flight were noticeable. Fig. 9 shows an image for PP at 8D.

Two more images for HDPE were captured at 10D from the video on one side of the screw flight, namely, the melt pool side, and they are presented in Fig. 6. The HDPE material was appreciably molten in this barrel position. Since the melt pool was transparent, the screw root and even its curvature were observed. With regard to solids bed profile, this measurement is equivalent to X/W << 1. Fig. 7 shows one image at 10D on the other side of the screw flight, namely, the solid bed side. From the left to the right, the screw flight, molten material and solid bed were clearly identified. It is noticeable that the amount of molten material on this side of the flight was wider in this position than in previous position L/D=8. The PP material at 10D showed more quantity of melt than solid and the high elasticity of the melt and screw flight were noticeable. Fig. 10 shows an image for PP at 10D.

At L/D=12 both polymer materials were completely molten. The image looked like an empty screw due to the high transparency of the melt. Considering the solids bed profile, this measurement is equivalent to X/W = 0.

Solids bed profiles (SBP) could be obtained for the experiments at 10, 20, 30 and 40 rpm. Table 1 shows the experimental values of X/W versus L/D for HDPE to be compared with melting models and additional experimental observations.

A primary finding of these measurements is a full description of the mechanisms that take place during melting. In our observations, melting begins when the granules near the barrel surface approach the melting temperature, at which point the melt is smeared across the whole surface. It is observed that as melting progresses the formation of the melt pool is delayed for a few turns due to the fact that before a melt pool forms, the melt fills the gaps between the granules. This is in agreement with Tadmor and Agassant [19], who actually never measured this 'delay zone' but proposed its existence. In the present research, this delayed zone has been clearly observed. The filling of the porous regions between polymer granules is equivalent to a solid bed melt saturation process. This melt saturation or seepage probably occurs from all four sides, but primarily from the barrel surface side, where most of melt is generated. Once the solid bed is fully saturated the melt pool starts to grow on the channel side with lowest pressure, since the natural tendency of the solid bed region is to be pushed against the leading flight, or region of highest pressure.

The images taken at one position during one set of processing conditions, can be assembled as a mosaic to visualize the state of melt throughout the whole circumference of the extruder. This is equivalent to unwrapping an extruder slice, the width of a quartz window. Fig. 11 represents the position L/D=8 inside the solid bed melt saturation delay zone. The figure clearly demonstrates that the solid bed is fully covered by a melt film that extends over the screw flight. Fig. 12 shows from top to bottom the screw flight, the melt pool and the solid bed during the solid bed reduction process, after the saturation delay zone.

If we compare the experimental results with Tadmor's models and do not include the delay caused by the solid bed melt saturation process, as is done today, the analytical and the experimental results do not agree, as shown in Fig. 13. However if Tadmor's model is modified, such that the melt pool grows after experimentally determined delay zone, and not when the melt film first forms, the experimental results and modified model agree quite well, as shown in Fig. 14.

In these experiments, PP showed a higher viscoelastic behavior in the molten state than HDPE. It could be also observed that PP was very sticky against the quartz windows, as shown in Fig. 15, specially above its melt temperature. This occurrence has been also reported by some authors in the literature. Fig. 15 shows an image for PP at 12D, where the molten material is against the quartz window.

Conclusions

The optical technique used to analyze polymer melting proved successful for studying single screw extruders. It was possible to distinguish between granules, solid bed and molten material in the screw channel due to the differences in optical properties between the melt and the solid. HDPE and PP as semi crystalline materials were white and opaque as a solid and totally transparent in the molten state.

The presented and patented non-invasive technique (U.S Patent No. 7314363) allowed visualization and InLine-measurements of solid bed width and melt pool width in z-direction and can also provide direct observation of different polymer melting behavior inside extruders, [20, 21]. Therefore, solid bed profiles could be measured and be compared with Tadmor's analytical melting models. The extruder heat transfer was not affected in this case due to the small diameter of the boroscope holder opposite to the 'push-out' technique, [18] and the glass extruder technique, [10, 11]. The important finding of this research is a full description of the mechanisms that take place during melting. Melting begins when the granules near the barrel surface approach the melting temperature. At this point the melt is smeared across the whole surface. It is observed as melting progresses that the formation of the melt pool is delayed for a few turns due to the fact that before a melt pool forms, the melt fills the gaps between the granules. This is in agreement with Tadmor and Agassant [19], who actually never measured this 'delay zone' but proposed its existence. This delayed zone has been clearly observed. The filling of the porous regions was called solid bed melt saturation process. This melt saturation or seepage probably occurs from all four sides, but primarily from the barrel surface side, where most of melt is generated. Once the solid bed is fully saturated the melt pool starts to grow on this channel side with lowest pressure, as the natural tendency of the solid bed region is to be pushed against the leading flight, or region of highest pressure.

The formation of a thin melt layer on the passive flight allows inferring that the solid bed is surrounded by molten polymer but the actual optical technique does not allow this visualization and measurement.

Tadmor's melting model was modified, such that the melt pool grows after the experimentally determined delay zone, and not when the melt film first forms, the experimental results and modified model agree quite well.

All the obtained video images allowed a better understanding of polymer melting in extruders and the mechanisms involved like granules conveying, solid bed compaction, melt formation, solid bed melt saturation, decrease of solid bed, solid bed break-up and finally, elasticity and/or stickiness of the melt. The videos have a high educational value in polymer extrusion or polymer processing and are useful for troubleshooting.

References

/1/ B. H. Maddock, A Visual Analysis of Flow and Mixing in Extruder Screws, SPE- Journal 15 (1959), pp. 383 – 389
/2/ L.F. Street, Plastifying Extrusion, International Plastics Engineering, Vol. 1, (1961), pp. 289-296
/3/ Tadmor, Z., "Fundamentals of Plasticating Extrusion: A Theoretical Model for Melting", Polymer Engineering and Science, Vol. 6, pp. 185 - 190, 1966
/4/ Tadmor, Z., Duvdevani, I.J. and Klein, I., "Melting in Plasticating Extruders- Theory and Experiments", Polymer Engineering and Science, Vol. 7, pp. 198 – 217, 1967
/5/ Tadmor, Z. and Klein, I., "Engineering Principles of Plasticating Screw Extrusion", Van Nostrand Reinhold, New York, 1970
/6/ Shapiro, J. and Pearson, J.R.A., "A dynamic model for melting in plasticating extruders", Imperial College, Polymer Engineering Science Group, Report No 5, April, 1974
/7/ Shapiro, J., Halmos, A.H., and Pearson, R.A. "Melting in single screw extruders", Polymer, Vol. 17, pp. 905-918, 1976.
/8/ Shapiro, J., Halmos, A.L. and Pearson, J.R.A., "Melting in single screw extruders", Polymer, Vol. 17, pp. 905-918, 1976
/9/ Halmos, A.L., Pearson, J.R.A. and Trottnow, R. "Melting in single screw extruders", Polymer, Vol. 19, pp. 1199-1216, 1978
/10/ Wong, A.C.Y., Zhu, F., Liu, R. and Liu, T., "Breakup of solid bed in melting zone of single screw extruder. Part 1-Mathematical model", Plastics, Rubber and Composites Processing and Applications, Vol. 26, pp. 336-342, 1997
/11/ Wong, A.C.Y., Zhu, F., Liu, R. and Liu, T., "Breakup of solid bed in melting zone of single screw extruder. Part 2 - Strength of solid bed and experimental results", Plastics, Rubber and Composites Processing and Applications, Vol. 26, pp. 343-350, 1997
/12/ Derezinski, S., "A melting rate model based on extrusion data", SPE ANTEC'99, Vol. 1, pp.184 – 187, 1999
/13/ Bruker, I. and Balch, G.S., "Melting mechanism in single screw extrusion", Polymer Engineering and Science, Vol. 29, pp. 258-267, 1989.
/14/ Amellal, K. and Lafleur, P.G., "Computer simulation of conventional and barrier screw extruders", Plastics, Rubber and Composites Processing and Applications, Vol. 19, pp. 227-239, 1993
/15/ Huang, H. and Peng, Y., "Theoretical modeling of dispersive melting mechanism of polymers in an extruder", Advances in polymer technology, Vol. 12, pp. 343-352, 1993
/16/ Rauwendaal, C., "Comparison of two melting models", Advances in Polymer Technology, Vol. 15, No. 2, pp. 135-144, 1996
/17/ Ferrier, N., "Video Imaging of Extruder Melting", email communication, ME- University of WisconsinMadison 2001.
/18/ Tadmor, Z. and Gogos, C., "Principles of Polymer Processing", John Wiley and Sons, Inc., 1979
/19/ Agassant, J.F. et. al., "Polymer Processing: Principles and Modeling", Hanser Publishers, Munich, Germany, pp. 173, 1991
/20/ Noriega, María del Pilar, et. al., "Method and device to visualize in-line and quantify the polymer melting in plasticating screw machines without significantly affecting its thermal regime", U.S Patent No. 7314363, January 1, 2008.
/21/ Noriega, María del Pilar, et. al., "Dispositivo para visualizar en línea y método para cuantificar la fusión de polímeros en máquinas de plastificación con tornillo sin afectar significativamente su régimen térmico", Colombian patent No.15348,

March 31, 2009.

Acknowledgments

Thanks are also due to the Instituto de Capacitación e Investigación del Plástico y del Caucho (ICIPC) in Medellín, Colombia and COLCIENCIAS for their financial support to develop this research project.

Nomenclature

D Extruder diameter
L/D Extruder length
W Channel width
X Solid bed width
SBP Solids bed profile

Key Words: Single screw extruder, polymer melting, delay zone, HDPE, PP

L/D	X/W – 10 rpm	X/W - 20 rpm	X/W – 30 rpm	X/W – 40 rpm
6	1	1	1	1
8	0.86	Melt film saturation	Melt film saturation	Melt film saturation
10	0.36	0.73	Melt film saturation	Melt film saturation
12	0	0.48	0.69	0.75
14		0	0.28	0.56
16			0	0.44
18				0

Table 1: Experimental values of X/W vs. L/D for HDPE

Figure 1: Holder shell with quartz window

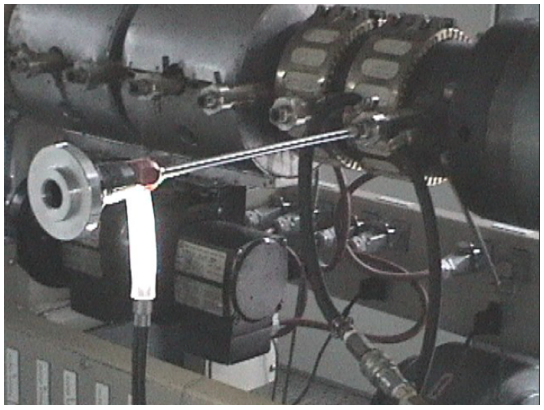

Figure 2: Extruder setup with holders and rigid boroscope

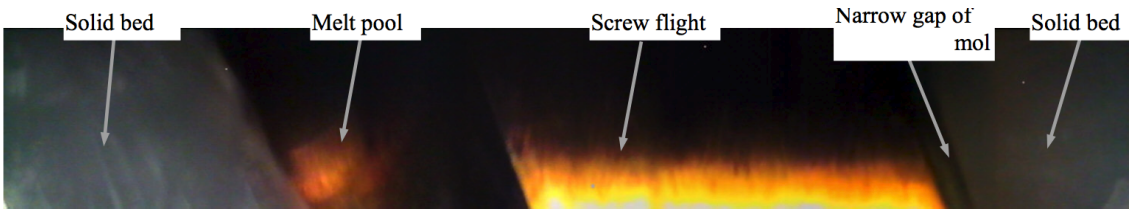

Figure 3: Image of the solid bed, melt pool and screw flight from inside the extruder

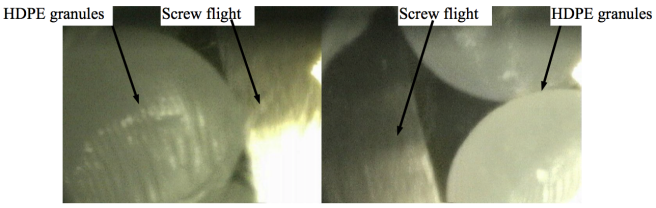

Figure 4: Images for HDPE at 10 rpm and L/D=6

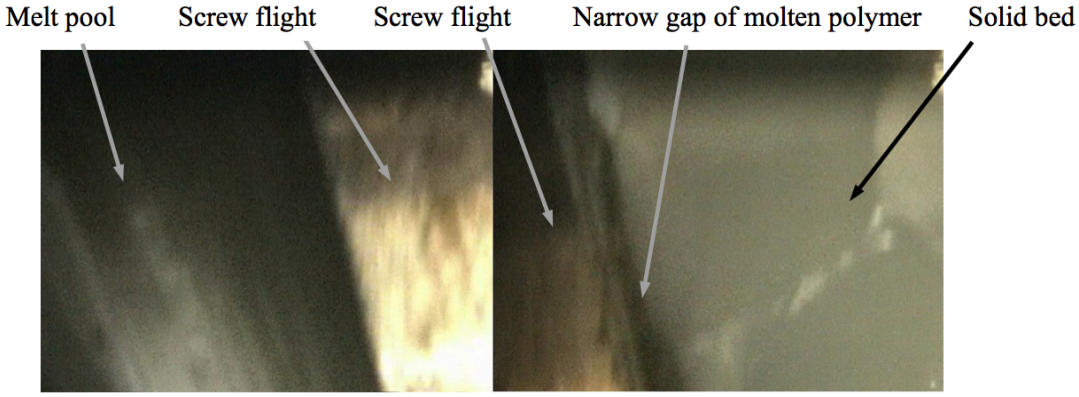

Figure 5: Images for HDPE at 10 rpm and L/D=8

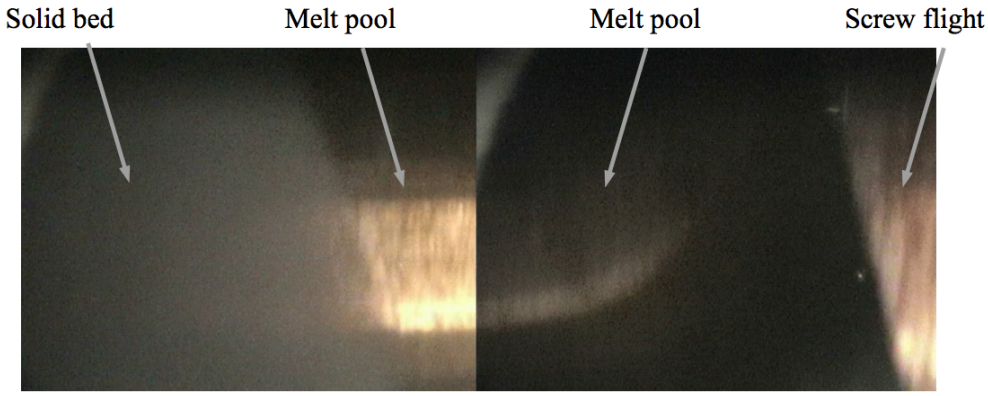

Figure 6: Images for HDPE at 10 rpm and L/D=10 on melt pool side

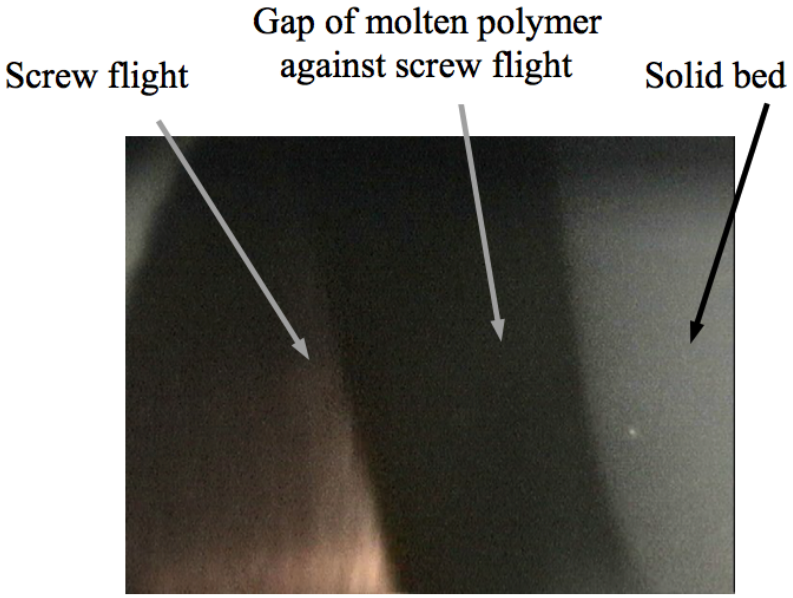

Figure 7: Image for HDPE at 10 rpm and L/D=10 on the other screw flight side

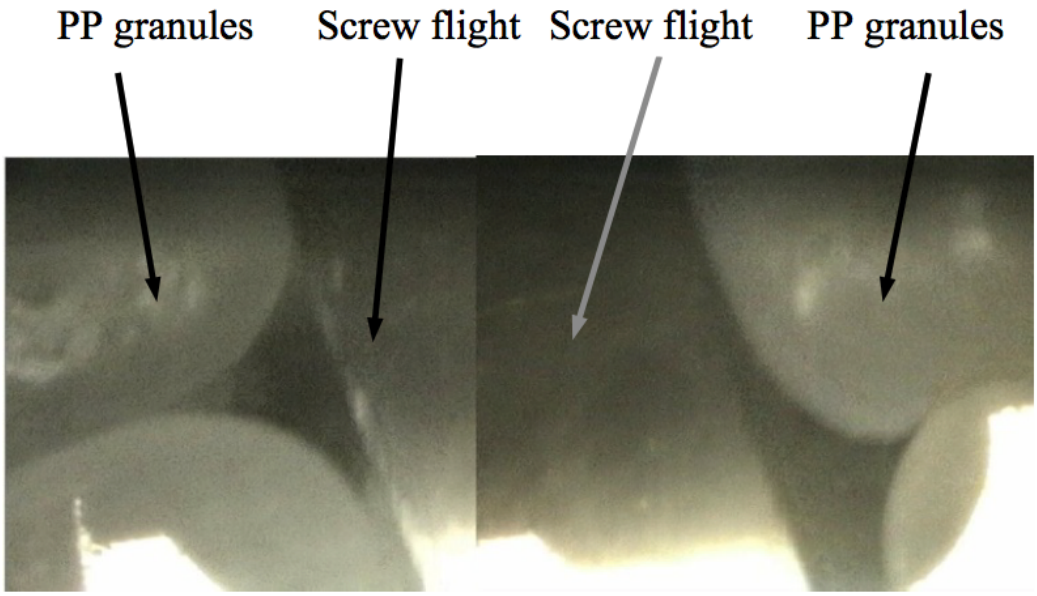

Figure 8: Images for PP at 10 rpm and L/D=6


Figure 9: Image for PP at 10 rpm and L/D=8

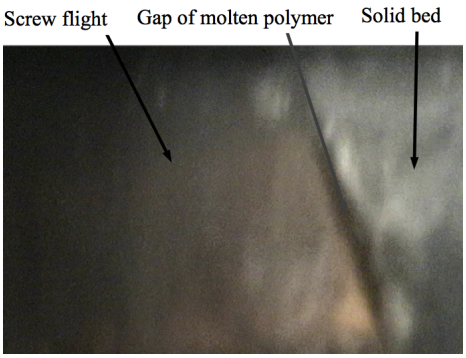

Figure 10: Image for PP at 10 rpm and L/D=10

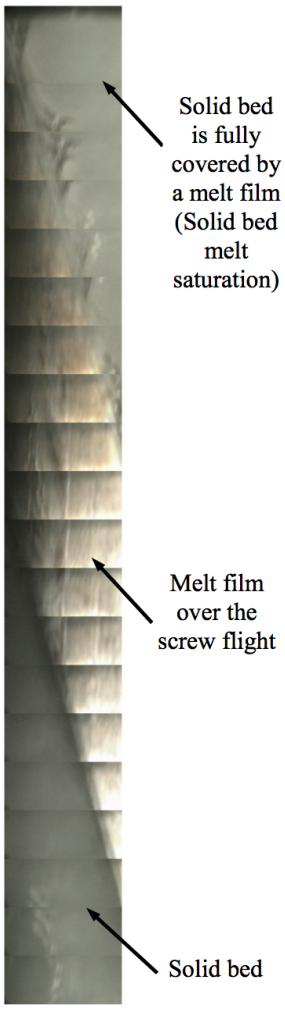

Figure 11: Mosaic of individual photos for HDPE at 20 rpm and L/D=8, 'Delay Zone'

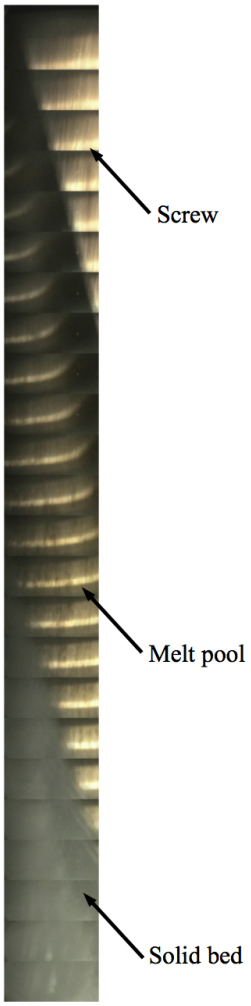

Figure 12: Mosaic of individual photos for HDPE at 20 rpm and L/D=10

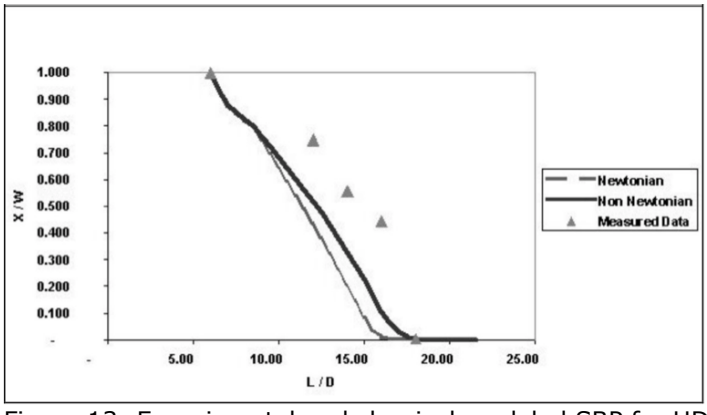

Figure 13: Experimental and classical modeled SBP for HDPE at 40 rpm

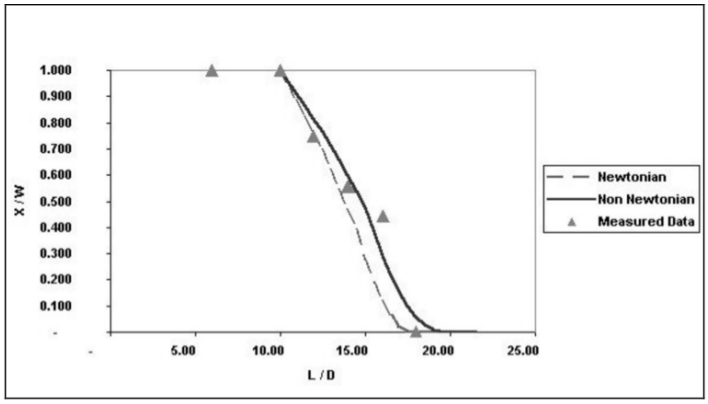

Figure 14: Experimental and modified modeled SBP for HDPE at 40 rpm

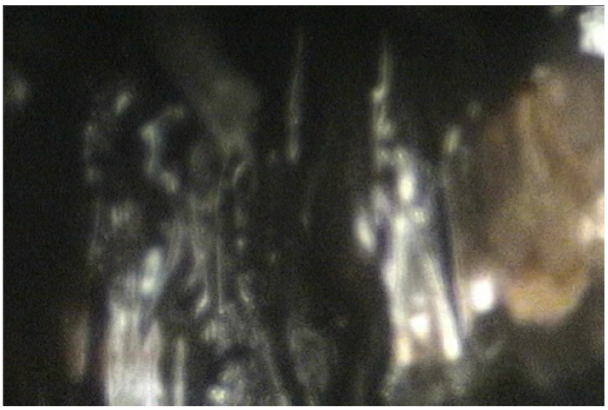

Figure 15: Image for PP at 10 rpm and L/D = 12

Return to Paper of the Month.